arXiv:1007.3988v2 [astro-ph.CO] 25 Aug 2010

CENTRAL DARK MATTER TRENDS IN EARLY-TYPE GALAXIES FROM STRONG LENSING, DYNAMICS AND STELLAR POPULATIONS

C. Tortora[1], N.R. Napolitano[2], A.J. Romanowsky[3], P. Jetzer[1]
(Received; Revised; Accepted)
Draft version August 26, 2010

ABSTRACT

We analyze the correlations between central dark matter (DM) content of early-type galaxies and their sizes and ages, using a sample of intermediate-redshift ($z \sim 0.2$) gravitational lenses from the SLACS survey, and by comparing them to a larger sample of $z \sim 0$ galaxies. We decompose the deprojected galaxy masses into DM and stellar components using combinations of strong lensing, stellar dynamics, and stellar populations modeling. For a given stellar mass, we find that for galaxies with larger sizes, the DM fraction increases and the mean DM density decreases, consistently with the cuspy halos expected in cosmological formation scenarios. The DM fraction also decreases with stellar age, which can be partially explained by the inverse correlation between size and age. The residual trend may point to systematic dependencies on formation epoch of halo contraction or stellar initial mass functions. These results are in agreement with recent findings based on local galaxies by Napolitano, Romanowsky & Tortora (2010) and suggest negligible evidence of galaxy evolution over the last ~ 2.5 Gyr other than passive stellar aging.

Subject headings: dark matter – gravitational lensing – galaxies : evolution – galaxies : galaxies : general – galaxies : elliptical and lenticular, cD.

1. INTRODUCTION

Early-type galaxies (ETGs) are among the most massive systems in the Universe. They are on average metal-rich, dust and gas poor, and formed their stars in early, rapid events (e.g., Thomas et al. 2005; Fontanot et al. 2009). The lack of easily interpretable dynamical tracers, such as the cold gas in spiral galaxies, has made the mass mapping of these systems very difficult in the outer regions where dark matter (DM) is expected to be dominant, although discrete tracers (planetary nebulae and globular clusters; e.g., Napolitano et al. 2009; Romanowsky et al. 2009) are providing a clearer view of the DM halos. The mass content of these galaxies' central regions has on the other hand been extensively investigated (e.g., Gerhard et al. 2001; Cappellari et al. 2006; Tortora et al. 2009, T+09 hereafter), with building evidence that the central DM fraction (f_{DM}) is an increasing function of total stellar mass ($M_\star$), providing the main driver for the tilt of the fundamental plane (e.g., T+09).

New insights into the galaxy assembly process are emerging from joint analyses of the structural and star formation properties of nearby ETGs (e.g., Gargiulo et al. 2009; Graves & Faber 2010; Napolitano, Romanowsky & Tortora 2010, NRT10 hereafter). A key discovery of NRT10 is an anti-correlation between f_{DM} and galaxy stellar age, such that older galaxies (at a fixed $M_\star$) have lower f_{DM}. In the context of ΛCDM halos, this trend can be partially explained by an anti-correlation between galaxy sizes and ages, with the remaining effect apparently driven by variations in star formation efficiency, stellar initial mass function (IMF), or DM distribution (e.g., adiabatic contraction, AC hereafter). As discussed in NRT10, such correlations would have deep implications for the assembly histories of ETGs, but critically need to be confirmed by independent analyses.

Gravitational lenses offer a unique tool to map the mass profile in galaxies over a range of redshifts. The database of lenses is growing quickly thanks to ongoing surveys (e.g., SLACS: Auger et al. 2009, A+09 hereafter; COSMOS: Faure et al. 2008). In particular, the SLACS survey has collected $\gtrsim 80$ secure lenses, which is a sample comparable to the total number of lenses discovered since the late 70s from other campaigns or by serendipity (e.g. Covone et al. 2009). Here, we will use the SLACS sample data to extend the analysis of NRT10, using both lensing and dynamics as independent probes of total mass, and providing a higher-redshift ($z \sim 0.2$) comparison to the $z \sim 0$ galaxies previously studied[4].

2. DATA SAMPLE AND ANALYSIS

2.1. *Galaxy Samples*

The lensing galaxy sample is taken from the SLACS survey (A+09)[5], which has been extensively analyzed in other works (e.g., Bolton et al. 2006, 2008; Gavazzi et al. 2007; Cardone et al. 2009; Treu et al. 2010; Grillo et al. 2009; Cardone & Tortora 2010). The lens galaxy redshift (z_l) range is $0.05 \leq z_l \leq 0.5$, with a median of $z_l \sim 0.2$. Our sample is selected: 1) to have a measured Einstein radius R_E[6] in Table 3 of A+09, 2)

Electronic address: ctortora@physik.uzh.ch
[1] Universität Zürich, Institut für Theoretische Physik, Winterthurerstrasse 190, CH-8057, Zürich, Switzerland
[2] INAF – Osservatorio Astronomico di Capodimonte, Salita Moiariello, 16, 80131 - Napoli, Italy
[3] UCO/Lick Observatory, University of California, Santa Cruz, CA 95064, USA

[4] In the paper, we use a cosmological model with $(\Omega_m, \Omega_\Lambda, h) = (0.3, 0.7, 0.7)$, where $h = H_0/100\,\mathrm{km\,s^{-1}\,Mpc^{-1}}$ (Spergel et al. 2007), corresponding to a universe age today of $t_{univ} = 13.5$ Gyr.

[5] See also http://www.slacs.org/

[6] The Einstein radii are derived by fitting a singular isothermal ellipsoid (SIE) profile and are quoted adopting an intermediate-axis normalization. Five of the galaxies without a measured R_E

to be classified as elliptical or S0, 3) to have a measured V-band effective radius (measured at the intermediate axis). Of the 85 lenses from this latest SLACS release, 66 passed our selection criteria.

As a $z \sim 0$ comparison sample, we use the collection of 330 ETGs over the same mass range analyzed in T+09 and NRT10.

2.2. *Stellar population analysis*

To estimate stellar mass-to-light ratios ($\Upsilon_\star$) and star formation histories, we analyze spectral energy distributions (SEDs) based on broad-band Sloan Digital Sky Survey (SDSS) photometry (namely, $ugriz$). Our general procedure is to adopt a set of synthetic spectra from the prescription of Bruzual & Charlot (2003), a uniform metallicity Z, an age t characterizing the time of star formation onset, and an exponentially declining star formation rate with timescale τ. For each galaxy, Z, t, and τ are fitted parameters, with the determined $\Upsilon_\star$ based on a Kroupa (2001) IMF; uncertainties on the estimated parameters have been quantified via Monte Carlo simulations: further details are provided in T+09 and NRT10 along with explorations of systematic uncertainties and degeneracies. The only change here is to shift the spectral responses of the SDSS filters to correspond to the lens redshifts before convolving with the model SEDs. We have checked that imposing restrictions on Z or τ, or adopting the stellar populations results from A+09 or Grillo et al. (2009), does not qualitatively affect the results described below.

2.3. *Total mass and dark matter content*

We derive the deprojected total mass from dynamics and lensing observables, and separate the DM from the stellar components using the stellar mass estimates discussed in the previous section. We adopt the stellar effective radius $R_{\rm eff}$ as the fiducial reference point for mass comparisons. For the lens galaxies, $R_{\rm eff}$ is measured in the V-band, corresponding approximately to the rest-frame B-band used for the local galaxies. In both galaxy samples, the mass constraints are generally based on measurements at smaller radii ($\sim 0.1R_{\rm eff}$ and $\sim 0.5R_{\rm eff}$, respectively), and therefore some extrapolation is required. For the total mass distribution we adopt a singular isothermal sphere (SIS) with density $\rho(r) = \sigma_{\rm SIS}^2/(2\pi G r^2)$ (e.g. Koopmans et al. 2006, Gavazzi et al. 2007, Koopmans et al. 2009), where $\sigma_{\rm SIS}$ is an unknown normalization to be determined by fitting the observables. For the stars, we adopt a constant-Υ_* mass profile based on the Hernquist (1990) model.

To estimate dynamical masses we have used the SDSS stellar velocity dispersions $\sigma_{\rm SDSS}$, measured within a circular aperture of $R_{\rm ap} = 1.5''$. Briefly, we have adopted the spherical Jeans equation to derive the surface brightness weighted velocity dispersion $\sigma_{\rm ap,SIS}$ within $R_{\rm ap}$ (see T+09 for further details), to be matched to $\sigma_{\rm SDSS}$. As discussed in T+09, there is some degree of systematic uncertainty from assumptions of sphericity and orbital isotropy, which we can now check in the case of the lenses by using the independent lensing-based masses (which do

have a nearby companion while, for other systems, the HST data do not have sufficient sensitivity to adequately perform the lensing model.

have their own uncertainties from mass-sheet degeneracies).

For the lensing mass estimates, we have used the Einstein radius $R_{\rm E}$, to derive a model independent measurement of projected mass ($M_{\rm proj}$) within $R_{\rm E}$, since $M_E = M_{\rm proj}(R_{\rm E}) = \pi R_{\rm E}^2 \Sigma_{\rm crit}$, where $\Sigma_{\rm crit} = c^2 D_s/4\pi G D_l D_{ls}$, with D_s, D_l and D_{ls} the observer - source, observer - lens and lens - source comoving angular diameter distances, respectively. Finally we match the prediction of the SIS model projected mass, $M_{proj,SIS}$ with M_E to have a further constraint on the only free model parameter for each galaxy, $\sigma_{\rm SIS}$.

The best fitted $\sigma_{\rm SIS}$ can be derived independently using either technique to estimate the best 3D deprojected mass profile which we extrapolate to $r = R_{\rm eff}$ to obtain our reference mass values. Using this approach, we find that lensing and dynamics provide consistent results, modulo a $\sim 10\%$ (and a scatter of $\sim 25\%$) higher mass from dynamics, corresponding to a change of 0.03 ± 0.10 in $f_{\rm DM}$. Thus, we adopt a combination of the constraints for our final masses, by minimizing with respect to $\sigma_{\rm SIS}$ a combined χ^2 function including one term for dynamics and one for lensing observables, given by

$$\chi^2 = \left(\frac{\sigma_{ap} - \sigma_{SDSS}}{\delta_d}\right)^2 + \left(\frac{M_E - M_{proj,SIS}}{\delta_l}\right)^2, \quad (1)$$

where δ_d and δ_l are the uncertainties on $\sigma_{\rm SDSS}$ and M_E, respectively [7].

In the following we will focus on the central 3D deprojected $f_{\rm DM}$ and the mean DM density within $R_{\rm eff}$, defined as $\langle\rho_{\rm DM}\rangle = M_{\rm DM}/(4/3\pi R_{\rm eff}^3)$ where $M_{\rm DM} = M_{\rm tot} - M_\star$ at $R_{\rm eff}$ is the DM mass.

2.4. *Cosmological models*

As in T+09 and NRT10, to interpret the observational results, we construct a series of toy mass models based on ΛCDM cosmological simulations. For each bin in $M_\star$, we use the average $R_{\rm eff}$-age relations from the combined lens+local sample, and parameterize the virial DM mass by a star formation efficiency $\epsilon_{\rm SF} = M_\star/(\Omega_{\rm bar}M_{\rm tot})$, where $\Omega_{\rm bar} = 0.17$ (Spergel et al. 2007) is the baryon density parameter. The halo densities are initially characterized as Navarro et al. (1997) profiles following an average mass-concentration relation, adjusted by $(1+z)^{-1}$ for the lens galaxies. A recipe for AC from baryon settling is then applied (Gnedin et al. 2004). The toy models for $\epsilon_{\rm SF} = 0.03, 0.1, 0.3$ are shown in both Figs. 1 and 3.

3. RESULTS: CORRELATIONS WITH SIZE AND FORMATION EPOCH

In order to marginalize any correlations with $M_\star$, we group the galaxies from both samples into bins of common median mass: $\log M_*/M_\odot \sim 11.6$, 11.3 and 10.9. For the lens galaxies, the corresponding median redshifts are $z_{\rm med} = 0.28, 0.18, 0.13$. The local galaxies sample extends to even lower masses ($\log M_*/M_\odot \sim 10.4$) with no lens counterparts.

---

[7] Note that δ_d is given in Table 3 of A+09 and ranges from 2% to 19% (with mean 6%), while we have assumed a nominal 5% uncertainty on $R_{\rm E}$ which corresponds to a relative error of 10% on M_E. However, the results are qualitatively unchanged if we would assume $\delta_d = \delta_l$.
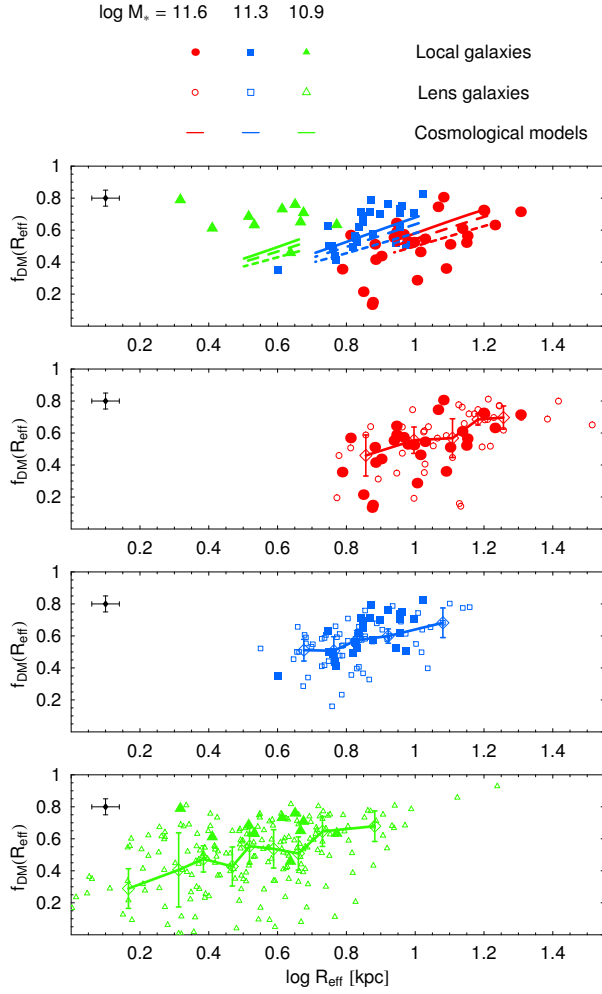
FIG. 1.— Dark matter fraction within an effective radius ($R_{\rm eff}$) as a function of $R_{\rm eff}$. The lens and local galaxies are shown as filled and open symbols, respectively. For the latter, open symbols with error bars show the median and $\pm 25\%$ values. Typical 1σ uncertainties for individual galaxies are shown to the left. The differently colored symbols denote different bins of stellar mass, as labeled in the legend in the top. The second panel from the top shows the combined bins for the lens galaxies only and includes toy-model ΛCDM predictions: solid, long-dashed, and short-dashed curves show star formation efficiencies of $\epsilon_{\rm SF} = 0.03, 0.1, 0.3$, respectively.

Our first result (which we do not show for the sake of space) is that for the lenses, $f_{\rm DM}$ increases on average with $M_\star$ (see Cardone et al. 2009 and Cardone & Tortora 2010 for details). This result confirms that as in local galaxies (T+09), $f_{\rm DM}$ is also a main driver of the fundamental plane tilt at $z \sim 0.2$.

Next, following NRT10, we focus on correlations of the DM metrics with galaxy size and age. For the latter we adopt the look-back time to the formation epoch in order to put all the galaxies with different observed redshifts on a common reference frame.

Fig. 1 demonstrates that there is a strong positive correlation between $f_{\rm DM}$ and $R_{\rm eff}$, once the galaxies are divided into mass bins. This may be understood as a larger $R_{\rm eff}$ enclosing a bigger portion of the DM halo; this "aperture effect" appears to be more dominant than the $f_{\rm DM}$ correlation with $M_\star$. The local and lens samples
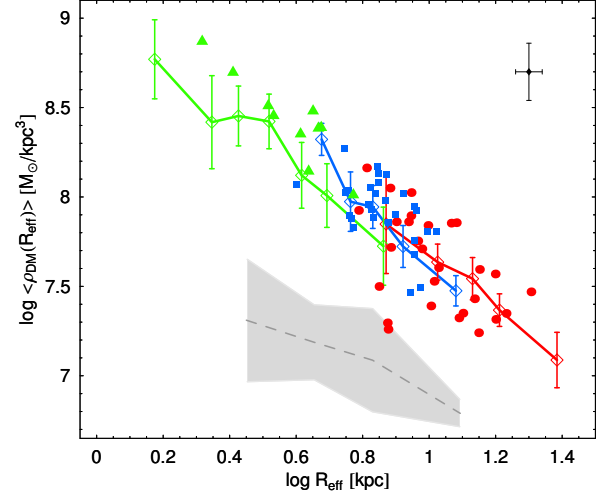

FIG. 2.— Mean DM density within 1 $R_{\rm eff}$ as a function of $R_{\rm eff}$. See Fig. 1 for the meaning of symbols. The grey region shows an average of spiral galaxy results from McGaugh et al. (2007).

appear reasonably similar, although the lens galaxies in the lowest mass bin are systematically higher, which is an issue we will discuss below. Both samples are in rough agreement with our ΛCDM toy model predictions (top panel).

Fig. 2 shows that $\langle \rho_{\rm DM} \rangle$ strongly anti-correlates with $R_{\rm eff}$. Again considering the aperture effect and assuming DM halo homogeneity, the implication is that we are measuring a mean DM density profile with radius, with a best fitted log slope of ~ -1.7. As discussed in NRT10, this steep slope is indicative of cuspy halos, perhaps as induced by AC. One could suspect that we are getting out what we are putting in, since our default galaxy model assumes an isothermal total density profile (with slope ~ -2) in order to extrapolate measurements to $r = R_{\rm eff}$, but we have shown in NRT10 that the use of an alternative constant-M/L profile yields similar results (modulo a difference of $0.1 - 0.2$ in the slope), still fully consistent with a cuspy contracted halo[8].

In Fig. 2, we also see that the ETGs have DM densities substantially larger than those of local spiral galaxies, which have been suggested to follow a unified halo trend with dwarf spheroidals (Donato et al. 2009; Walker et al. 2010). This dichotomy is qualitatively consistent with other findings (Gerhard et al. 2001; Thomas et al. 2009; NRT10; Cardone & Tortora 2010), and may imply different formation mechanisms. The difference might be assumed as simply caused by ETGs forming from denser late-type galaxies at earlier epochs, which would yield the corollary prediction that ETGs with younger stellar ages have less dense halos because their late-type progenitors were less dense. However, as we will see below, the opposite trend appears to be observed.

Finally we consider the $f_{\rm DM}$-age dependencies in Fig. 3, again using separate $M_\star$ bins. The lens and local galaxies match up remarkably well in general, showing a clear trend for lower $f_{\rm DM}$ at older ages. The low-mass lens

_____

[8] Note that the two massive galaxies J0157−0056 and J0330−0020 with $\log R_{\rm eff} \sim 0.9$, which depart from the mean trend, are fitted by a possibly unrealistic supersolar metallicity; setting Z to the solar value, the galaxies' densities are incremented by 0.15 and 0.25 dex, respectively.
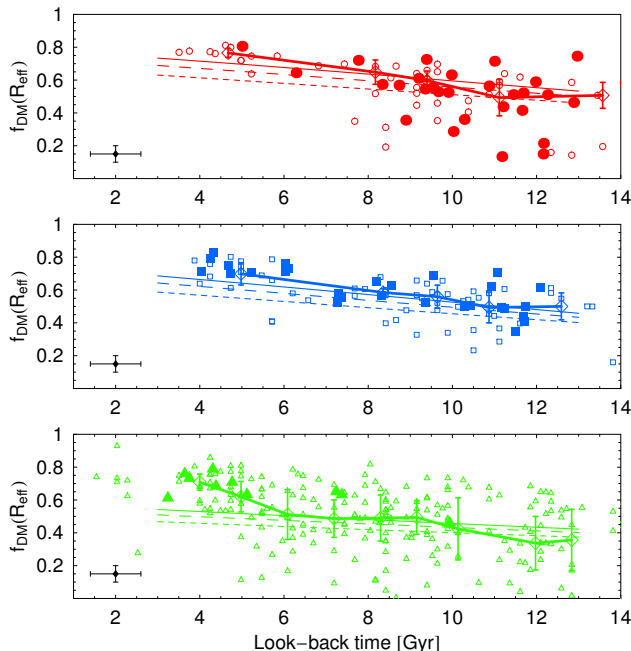
FIG. 3.— DM fraction within 1 $R_{\rm eff}$ as a function of galaxy stellar "age". See Figs. 1 and 2 for the meaning of symbols.

galaxies are predominantly young, which is probably a selection effect on apparent magnitude. The $f_{\rm DM}$-age anti-correlation then causes the overall $f_{\rm DM}$ for this mass bin to be high. In summary, at a fixed galaxy age and mass, the higher-z sample does not show any significant difference with the local galaxies. Since we have not applied any evolutionary corrections, the implication is that in the last ~ 2.5 Gyr (on average) the galaxy populations have experienced no measurable evolution except stellar aging[9].

We also include the ΛCDM toy models in Fig. 3, and see that some $f_{\rm DM}$-age anticorrelation is expected, which can be traced to the anti-correlation between $R_{\rm eff}$ and age. However, there are indications in every mass bin that the observed $f_{\rm DM}$-age slope is steeper than in the models. Some systematic link between age and $\epsilon_{\rm SF}$ is possible, but the models shown in Fig. 3 suggest that this would not be a strong enough effect, as changes in virial mass do not propagate strongly to changes in central DM content (and in fact earlier collapsing halos should have *denser* centers, which goes in the wrong way to explain the observations). The alternatives as discussed in NRT10 are that AC is more effective in younger galaxies, or that older galaxies have "lighter" IMFs (e.g., Kroupa versus Salpeter 1955 for the younger galaxies).

4. CONCLUSIONS

We have analyzed the central DM content of a sample of intermediate-z lenses from the latest release of the SLACS survey (A+09). Following the phenomenological framework introduced in T+09 and NRT10 we have

---

[9] Here the stellar mass bins can be biased at different redshifts due to the stellar population evolution and introduce a spurious tilt in the $f_{\rm DM}$-age relation. We have checked from the stellar models that the change in stellar mass due to stellar evolution might be not larger than ~ -0.01 in log $M_\star$ (due to mass loss), which makes our stellar bins at different z fairly homogeneous.

discussed scaling relations between DM fraction, galaxy size, and formation epoch. Gravitational lensing and dynamical analyses are used to constrain the total mass profile, while synthetic spectral populations are used to infer the stellar mass and other stellar properties such as galaxy age.

ETGs at $z \sim 0.2$ are found to be similar to local ones; future work will include extending the baseline to higher redshifts. The somewhat surprising findings of NRT10 are now confirmed with an independent and arguably more robust data set. The DM fraction within $R_{\rm eff}$ is found to strongly correlate with $R_{\rm eff}$, because larger length-scales probe a more DM dominated region. On these scales, the DM mean density decreases with $R_{\rm eff}$ as $\langle \rho_{\rm DM} \rangle \propto R_{\rm eff}^{-1.7}$, which argues for cuspy DM halos for ETGs out to $z \sim 0.5$ (as was discussed in NRT10 for local galaxies). At a fixed stellar mass and length-scale, we have found that the DM halos of ETGs are denser than those of local spiral galaxies, providing a critical test for the merging formation scenario (see also Cardone & Tortora 2010).

Finally, we have confirmed our earlier finding that central DM content anti-correlates with stellar age. The strength of this correlation appears to exceed what is expected from size-age effects. A fundamental connection between galactic structure and star formation history is implied, which we propose is a consequence of variations with formation epoch of either DM halo contraction or stellar IMF.

In future work, we plan to investigate the impact on these results of more complex total and DM galaxy profiles (e.g. Cardone et al. 2005, Tortora et al. 2007) along the lines of recent work in Cardone et al. (2009) and Cardone & Tortora (2010). New high-quality data are also expected with the advent of future surveys both in the local Universe and at larger redshifts. Such surveys will include larger samples of gravitational lenses along with more detailed spectroscopic information, and could be used to verify and extend the results presented here, providing a clearer picture of the physical processes of ETG assembly.

Note added in proof. During the final phase of this manuscript, there appeared closely related work from Auger et al. (2010a,b, A+10a and A+10b respectively, hereafter), using a combination of strong lensing, and stellar dynamics and populations, to analyze virtually the same lens-galaxy sample. A key point of agreement is that A+10a found the strongest non-trivial correlate with central $f_{\rm DM}$ is $R_{\rm eff}$, which we think demonstrates that size rather than mass variation is the main driver for the fundamental plane tilt.

A+10b also constructed ΛCDM models, adding constraints from weak lensing to break the degeneracies between $\epsilon_{\rm SF}$, IMF, and halo model (AC or no-AC). Given the same IMF and halo assumptions, they found SF values that are on average higher than both ours (e.g.

$\epsilon_{SF} \sim 0.3 - 0.4$ versus ~ 0.1 for Salpeter+no-AC), and typical values found in other studies. Although these differences may seem large, they involve relatively small changes in the central DM properties which could be driven by differences in the modeling methods. We considered three-dimensional DM masses within R_{eff}, while A+10b analyzed projected masses within $R_{eff}/2$ in combination with large-radius constraints from weak lensing, so a direct comparison is not straightforward. We hope to track down the reasons for these discrepant conclusions in future work.

A+10b found that a Salpeter+no-AC model is preferred over a Chabrier IMF (with or without AC) using direct model fits. Without weak lensing constraints, our modeling permits either Salpeter+no-AC or Kroupa+AC solutions (see NRT10 for further details), while our Figure 2 (or Figure 9 in NRT10) does provide indirect evidence for very cuspy halos with AC (and a Kroupa IMF). They also found that the IMF may become heavier with galaxy mass ($\eta > 1$ in their notation). We find that stellar age is the more important parameter in this context, but if an IMF-mass relation is demanded, then $\eta < 1$. This difference appears to be caused at least partially by different stellar populations models: although we found that varying these models did not alter the basic age trends, the mass trends are weaker and more sensitive to the models.

REFERENCES

Auger M. W., Treu T., Bolton A. S., Gavazzi R., Koopmans L. V. E., Marshall P. J., Bundy K. & Moustakas L. A. 2009, ApJ, 705, 1099 (A+09)
Auger, M. W., Treu, T., Bolton, A. S., Gavazzi, R., Koopmans, L. V. E., Marshall, P. J., Moustakas, L. A., & Burles, S. 2010a, ApJ, submitted (arXiv:1007.2880) (A+10a)
Auger, M. W., Treu, T., Gavazzi, R., Bolton, A. S., Koopmans, L. V. E., & Marshall, P. J. 2010b, ApJL, submitted (arXiv:1007.2409) (A+10b)
Bolton, A. S., Burles, S. Koopmans, L. V. E., Treu, T., Moustakas, L. A. 2006, ApJ, 638, 703
Bolton, A. S., Burles, S. Koopmans, L. V. E., Treu, T., et al. 2008a, ApJ, 682, 964
Bruzual, A. G. & Charlot, S. 2003, MNRAS, 344, 1000 (BC03)
Cappellari M. et al. 2006, MNRAS, 366, 1126
Cardone V. F., Piedipalumbo E. & Tortora C. 2005, MNRAS, 358, 1325
Cardone V. F., Tortora C., Molinaro R., Salzano V. 2009, A&A, 504, 769
Cardone V. F. & Tortora C. 2010, MNRAS, submitted (arXiv:1007.3673)
Covone, G. et al. 2009, ApJ, 691, 531
Donato, F. et al. 2009, MNRAS, 397, 1169
Faure C. et al. 2008, ApJS, 176, 19
Fontanot, F. et al. 2009, arXiv:0901.1130
Gargiulo, A., et al. 2009, MNRAS, 397, 75
Gavazzi, G., Bonfanti, C., Sanvito, G., Boselli, A., Scodeggio, M. 2002, ApJ, 576, 135G
Gavazzi, R. et al. 2007, ApJ, 667, 176G
Gerhard, O., Kronawitter, A., Saglia, R. P. & Bender, R. 2001, AJ, 121, 1936
Gnedin O. Y., Kravtsov A. V., Klypin A. A. & Nagai D. 2004, ApJ, 616, 16
Graves, G. J., & Faber, S. M. 2010, ApJ, submitted, arXiv:1005.0014

Grillo, C., Gobat, R., Lombardi, M., & Rosati, P. 2009, A&A, 501, 461
Hernquist, L. 1990, ApJ, 356, 359
Koopmans, L. V. E., Treu, T., Bolton, A. S., Burles, S., Moustakas, L. A. 2006, ApJ, 649, 599K
Koopmans L. V. E., et al. 2009, ApJ, 703, 51
Kroupa P., 2001, MNRAS, 322, 231
McGaugh, S. S., de Blok,W. J. G., Schombert, J. M., Kuzio de Naray, R. & Kim, J. H. 2007, ApJ, 659, 149
Napolitano, N. R., Romanowsky, A. J., Coccato, L., et al. 2009, MNRAS, 393, 329
Napolitano N. R., Romanowsky A. J. & Tortora, C. 2010, MNRAS, 405, 2351 (NRT10)
Navarro, J. F., Frenk, C. S., & White, S. D. M. 1997, ApJ, 490, 493
Romanowsky, A. J., Strader, J., Spitler, L. R., Johnson, R., Brodie, J. P., Forbes, D. A., & Ponman, T. 2009, AJ, 137, 4956
Salpeter, E.E. 1955 ApJ, 121, 161
Spergel, D. N., et al. 2007, ApJS, 170, 377
Thomas, J., Saglia, R. P., Bender, R., Thomas, D., Gebhardt, K., Magorrian, J., Corsini, E. M., Wegner, G. 2005, MNRAS, 360, 1355
Thomas, J., Saglia, R. P., Bender, R., Thomas, D., Gebhardt, K., Magorrian, J., Corsini, E. M. & Wegner, G. 2009, ApJ, 691, 770
Tortora C., Cardone V.F. & Piedipalumbo E. 2007, A&A, 463, 105
Tortora C. et al. 2009, MNRAS, 396, 1132 (T+09)
Treu, T., Auger, M. W., Koopmans, L. V. E., Gavazzi, R., Marshall, P. J. & Bolton, A. S. 2010, ApJ, 709, 119
Walker, M. G., McGaugh, S. S., Mateo, M., Olszewski, E., & Kuzio de Naray, R. 2010, ApJL, in press, arXiv:1004.5228